

The power available to tidal turbines in an open channel flow

Guy Tinmouth Houlsby MA, DSc, FEng, FICE
Professor of Civil Engineering, Department of Engineering Science,
University of Oxford, Oxford, UK

Christopher Reiner Vogel BE (Hons), DPhil
Research Assistant, Department of Engineering Science, University of Oxford,
Oxford, UK (corresponding author: christopher.vogel@eng.ox.ac.uk)

Linear momentum actuator disc theory is extended to address the power available to a tidal turbine array spanning the cross-section of an open channel flow. A generalised formulation is presented, which relaxes constraints in previous models on the Froude number of the flow and the geometry of the turbine array, and also considers the effects of far-wake mixing on the overall power removed from the flow. In the limiting case of no free surface deformation, the rigid lid model is recovered. Blockage, the ratio of turbine frontal area to the cross-sectional area of the surrounding flow passage, has the greatest effect on available power, with the peak power coefficient increasing by 55% from 0.60 to 0.93 as the blockage ratio increases from 0.05 to 0.20. A further 3% increase in peak power coefficient is achieved as the Froude number increases from 0.05 to 0.20. The efficiency of energy extraction may be determined relative to the total power extracted from the flow, comprising the power available to the turbines, and the power dissipated in wake mixing. Higher blockage turbines operating at low thrust coefficients are shown to be more efficient than lower blockage turbines.

Notation

A	cross-sectional area of the stream tube
B	blockage ratio
b	width of the flow passage
C_P, C_{PTot}	power coefficient, total power coefficient
C_T, C_{TL}	thrust coefficient, local thrust coefficient
E	total energy
Fr	Froude number
g	acceleration due to gravity
H	total head
h	static head
P, P_{Tot}	power
T	thrust
u	flow speed
$()_n$	variable at station n
α	non-dimensional core flow speed
β	non-dimensional bypass flow speed
Δh	difference in static head between stations 1 and 5
η	basin efficiency
ρ	water density

1. Introduction

Tidal power development has attracted significant interest over the past several decades as a potential source of predictable, renewable energy (Carbon Trust, 2007). The tide-generating

forces due to the relative position of the earth, moon and sun mean that the tides can be predicted with precision a long way into the future. The predictability of tidal power is seen as a particular advantage in the context of renewable energy, because it offers, in contrast to other renewable energy resources such as wind and solar, certainty about the power that is available for extraction at any point in time (Adcock *et al.*, 2015). This may be particularly advantageous in auxiliary services markets as renewable energy penetration increases.

Tidal power may be extracted by two main means: either through the use of tidal barrages to exploit the sea level difference at high and low tides or through deploying devices which can extract energy from tidal currents. Tidal barrage developments have been slowed by concern about their impacts on the environment due to the construction of embankments to impound seawater, either in a lagoon or in an estuary (Kirby and Retière, 2009). Tidal current turbines have therefore received considerable interest as an alternative technology with a potentially lower environmental impact. Recent estimates for the UK suggest that 29 TWh per year may be available from tidal stream energy, which represents about 10% of UK electricity demand (Carbon Trust, 2010). Commercialisation of tidal stream technology requires that the nature of the tidal stream resource, and how it can be harvested while minimising adverse effects on the environment, is better understood.

In particular, analytic tools, such as those derived herein, can help by providing quick analyses of the tidal resource and indicate upper bounds to the power available at tidal stream sites.

Linear momentum actuator disc theory (LMADT), introduced by Betz (1920) and Lanchester (1915), has been used to derive upper limits to the power that may be extracted from a fluid. Betz and Lanchester considered an actuator disc in an infinite volume of air to derive the well-known Lanchester–Betz limit (Betz, 1920; Lanchester, 1915) for a wind turbine, which limits power extraction to 59.3% of the undisturbed kinetic flux through the actuator disc. As the atmospheric flow of air is less constrained than that of a liquid in an open channel, a stream tube around a wind turbine will expand more freely than that around a tidal current turbine. The flow around the tidal current turbine is constrained by the much higher density of water than air, and by the proximity of the free surface. Therefore, the Lanchester–Betz limit is not directly applicable to tidal stream turbines (Bryden *et al.*, 2007).

Actuator disc models have been applied to tidal current turbines by Garrett and Cummins (2007), Houlsby *et al.* (2008) and Whelan *et al.* (2009). Garrett and Cummins (2007) considered a tidal turbine in a ‘rigid-lid’ channel – that is, a channel in which the free surface does not deform – which requires the Froude number of the flow to be sufficiently low for the solution to be accurate. It was shown that the blockage ratio, the ratio of the actuator disc frontal area to the cross-sectional area of the channel, was important in determining the peak power coefficient that could be achieved by the turbine, increasing the power coefficient by a factor of $(1 - B)^{-2}$ above the Lanchester–Betz limit (Betz, 1920; Lanchester, 1915). The model developed by Whelan *et al.* (2009) included the deformation of the free surface, but did not consider the mixing that must occur in the wake downstream of the turbine, which is required in order to determine correctly the total energy removed from the flow. This is particularly important in cases where the total power removed from the flow is regulated by, for example, environmental considerations, giving rise to the need to understand better both the efficiency of power extraction by the turbine itself and the efficiency of power extraction from the larger tidal flow. Houlsby *et al.* (2008) carried out a similar analysis but did include downstream mixing.

It is useful to distinguish between different definitions of the extracted power. The ‘available power’ is the power available to an actuator disc (which represents the inviscid upper limit of the shaft power of a tidal turbine (Adcock *et al.*, 2014)), whereas the total power removed from the flow, the ‘removed power’, accounts for both the available power and the power

dissipated in the mixing processes in the wake. The removed power is always greater than, or equal to, the available power due to the mixing that must occur in the wake downstream of the turbine. In the classic case of the Lanchester–Betz limit, the available power is 2/3 of the removed power.

This paper, based on the analysis of Houlsby *et al.* (2008), presents an analytic actuator disc model which includes the deformation of the free surface and the wake mixing downstream of the turbine to estimate more precisely the power available to a tidal turbine. In particular, the potential environmental and structural benefits of operating tidal turbines at points other than the peak power coefficient are explored. The effects of energy extraction on the larger-scale flow through an array of such turbines, or the tidal channel, are not considered here, but could be studied using the present model within a larger array or channel model.

2. Model

Figure 1 illustrates the inviscid, incompressible flow around a single actuator disc with frontal area A in a frictionless open channel with a flat seabed of constant width b . The authors use here the usual terminology of an ‘actuator disc’ which derives from the analysis of axial flow turbines which intercept a circular area of flow. The authors note, however, that their analysis (and that of Betz (1920)) makes no assumption about the shape of the device, and is equally applicable, for instance, to cross-flow devices that usually intercept a rectangular area. The flow speed $u_1 = u$ and static head $h_1 = h$ far upstream of the actuator disc at station 1 are taken as reference values in the following analysis. The flow is divided into two stream tubes as it approaches the actuator disc: the core flow, which encapsulates the flow through the disc, and the bypass flow, which contains the flow around the actuator disc. Station 2 is immediately upstream of the actuator disc, station 3 immediately downstream of the disc, station 4 is at an assumed position where the hydrostatic pressure can be considered as equal in the core and bypass flows, although the core and bypass flow speed are not yet equal. The two flows then mix, resulting in a new uniform flow speed and static head at station 5. Note the implicit assumption that pressure equalisation occurs over a much shorter length scale than mixing and speed equalisation.

The disc exerts a thrust T on the flow, resulting in a static head difference $h_{d2} - h_{d3}$ across the actuator disc. The flow speed in the core flow reduces to u_2 immediately upstream of the actuator disc. The core flow speed is also u_2 immediately downstream of the disc as it is assumed that the cross-sectional area of the core flow is the same across the disc. The flow speed in the disc wake at station 4 is u_{d4} as the core flow stream tube expands to a cross-sectional area of A_{d4} and the static head recovers to h_4 .

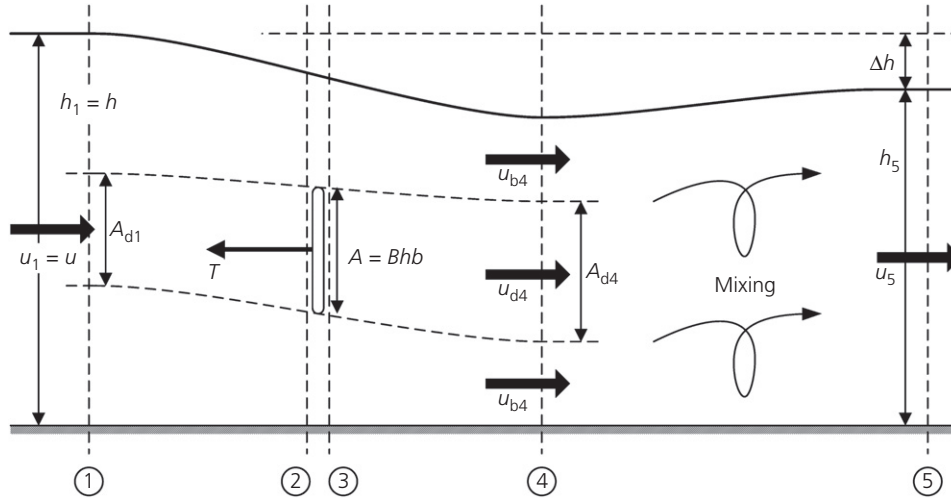


Figure 1. One-dimensional LMADT in an open channel flow

The bypass flow is accelerated from u_1 to u_{b4} to conserve mass flux through the bypass in response to the expanding core stream tube and the confinement of the flow due to the deformable free surface. The static head in the bypass reduces from h_1 to h_4 to conserve the total head in the bypass. The core and bypass flows then mix viscously between stations 4 and 5, yielding a new hydrostatic head h_5 and complementary uniform flow speed u_5 . The static head reduces by Δh between stations 1 and 5 as a result of energy extraction from a sub-critical flow, although this change in head is normally very small relative to the depth of the flow. The flow speed at the outlet of the channel is thus accelerated from u_1 to u_5 to maintain the mass flux through the channel.

The fact that the flow speed of a sub-critical flow increases as power is extracted confounds the usual (rather imprecise) statement that ‘tidal turbines extract kinetic energy from the flow’.

2.1 Model parameterisation

It is useful to define a number of non-dimensional groups describing the geometric ratios, actuator disc performance and the flow conditions in the actuator disc model. The velocities in the core flow are non-dimensionalised as $\alpha_i = u_{di}/u$ and in the bypass flow $\beta_i = u_{bi}/u$.

The concept of blockage, the ratio of the actuator disc frontal area to the cross-sectional area of the channel, can be introduced as follows

$$1. \quad B = \frac{\text{Turbine frontal area}}{\text{Channel cross-sectional area}} = \frac{A}{bh}$$

The thrust coefficient is defined by normalising the disc thrust by the upstream dynamic pressure projected onto the frontal area of the actuator disc

$$2. \quad C_T = \frac{T}{(1/2)\rho u^2 A}$$

A local thrust coefficient may be defined which parameterises the effect that the actuator disc has on the flow local to the disc, rather than the flow far upstream of the device. The local thrust coefficient is defined by normalising the thrust on the dynamic pressure acting on the frontal area of the disc

$$3. \quad C_{TL} = \frac{T}{(1/2)\rho u_2^2 A} = \frac{C_T}{a_2^2}$$

The power coefficient (elsewhere sometimes called the turbine efficiency) of the actuator disc is the product of the thrust and the flow speed through the disc, and is normalised by the kinetic flux of the upstream flow projected onto the actuator disc frontal area

$$4. \quad C_P = \frac{P}{(1/2)\rho u^3 A} = a_2 C_T$$

The total power, P_{Tot} , removed from the flow is the sum of the available power and the power dissipated in the wake mixing processes downstream of the actuator disc. Normalising the

total power by the kinetic flux of the upstream flow yields

$$5. \quad C_{PTot} = \frac{P_{Tot}}{(1/2)\rho u^3 A}$$

The concept of basin efficiency is also introduced to complement the traditional definition of turbine efficiency, represented here by the power coefficient. The basin efficiency is the fraction of the total energy removed from the flow that is extracted by the actuator disc, accounting for the additional loss of energy in the mixing region that is a consequence of the shearing between the faster bypass flow and the slower core flow

$$6. \quad \eta = \frac{\text{Available power}}{\text{Removed power}} = \frac{P}{P_{Tot}} = \frac{C_P}{C_{PTot}}$$

Finally, the upstream Froude number is introduced for the open channel flow as

$$7. \quad Fr = \frac{u}{\sqrt{gh}}$$

2.2 Model derivation

Conservation of energy is expressed by the Bernoulli equation between stations 1 and 2, and 3 and 4 in the core flow, and stations 1 and 4 in the bypass, requiring

$$8. \quad h + \frac{1}{2} \frac{u^2}{g} = h_{d2} + \frac{1}{2} \frac{u^2}{g} \alpha_2^2$$

$$9. \quad h_{d3} + \frac{1}{2} \frac{u^2}{g} \alpha_2^2 = h_4 + \frac{1}{2} \frac{u^2}{g} \alpha_4^2$$

$$10. \quad h + \frac{1}{2} \frac{u^2}{g} = h_4 + \frac{1}{2} \frac{u^2}{g} \beta_4^2$$

The thrust applied by the actuator disc to the flow is equal to the static head difference across the disc, integrated over the surface of the disc

$$11. \quad T = \rho g (h_{d2} - h_{d3}) B b h$$

Equations 8–10 may be rearranged for $h_{d2} - h_{d3}$, which is combined with Equation 11 to give an expression for the thrust in terms of the difference in the squares of the bypass and core velocities at station 4

$$12. \quad T = \frac{1}{2} \rho u^2 B b h (\beta_4^2 - \alpha_4^2)$$

Conservation of momentum between stations 1 and 4 requires the balance of the streamwise static head gradient, applied thrust and change in momentum of the fluid between stations 1 and 4

$$13. \quad \frac{1}{2} \rho g b (h^2 - h_4^2) - T = \rho u^2 b h (B \alpha_2) (\alpha_4 - 1) + \rho u^2 b h (1 - B \alpha_2) (\beta_4 - 1)$$

The static head terms in Equation 13 are eliminated by noting the requirement for conservation of mass across the water column between stations 1 and 4

$$14. \quad h_4 = \frac{B \alpha_2 h}{\alpha_4} + h \frac{(1 - B \alpha_2) h}{\beta_4}$$

in conjunction with Equation 10, which yields after some manipulation

$$15. \quad \left(1 + \frac{B \alpha_2}{\alpha_4} + \frac{(1 - B \alpha_2)}{\beta_4} \right) = \frac{2}{\beta_4^2 - 1} (2 B \alpha_2 (\alpha_4 - \beta_4) + 2 (\beta_4 - 1) + B (\beta_4^2 - \alpha_4^2))$$

Rearranging Equation 15 gives an expression for the non-dimensional flow speed through the actuator disc in terms of the non-dimensional velocities at station 4

$$16. \quad \alpha_2 = \frac{\alpha_4 (2 B (\beta_4^2 - \alpha_4^2) - (\beta_4 - 1)^3)}{B (\beta_4 - \alpha_4) (4 \alpha_4 \beta_4 + \beta_4^2 - 1)}$$

Combining Equations 10, 14 and 16 yields a quartic in β_4 in terms of α_4 , B and Fr

$$17. \quad \frac{1}{2} Fr^2 \beta_4^2 + 2 \alpha_4^2 Fr^2 \beta_4^3 - (2 - 2B + Fr^2) \beta_4^2 - (4 \alpha_4 + 2 \alpha_4 Fr^2 - 4) \beta_4 + \left(\frac{1}{2} Fr^2 + 4 \alpha_4 - 2 B \alpha_4^2 - 2 \right) = 0$$

If α_4 is specified and the flow is sub-critical, an exact solution to Equation 17 may be found. The appropriate root is determined by noting that $0 \leq \alpha_4 \leq \alpha_2 \leq 1$ and $\beta_4 \geq 1$ is required for a meaningful physical solution of the system of equations. This then allows the flow speed through the actuator disc, and thus the thrust and power coefficients, to be determined.

It is assumed that between stations 1 and 4 the interface between the core and bypass stream tubes can be treated as frictionless and therefore there is no mixing between the stream tubes. A shear stress is generated as a result of the difference in flow speed between the core and bypass flows, which drives the mixing process between stations 4 and 5. The two flows mix downstream of the hydrostatic pressure equalisation point at station 4, removing further energy from the flow to produce a uniform flow speed u_5 and water depth h_5 . The total removed power is therefore the sum of the energy extracted by the actuator disc (available power) and the power dissipated in the viscous mixing region in the wake.

The far-field effects of energy extraction by the actuator disc can be analysed by considering the conservation of momentum in the channel between stations 1 and 5, noting that continuity requires $h_1 u_1 = h_5 u_5$ and defining $\Delta h = h_1 - h_5$

$$18. \quad \frac{1}{2} \rho g b (h^2 - (h - \Delta h)^2) - T = \rho b h u \left(\frac{u h}{h - \Delta h} - u \right)$$

Equation 18 is cubic in the relative change in free surface elevation, $\Delta h/h$, in terms of the blockage, Froude number and thrust coefficient

$$19. \quad \frac{1}{2} \left(\frac{\Delta h}{h} \right)^3 - \frac{3}{2} \left(\frac{\Delta h}{h} \right)^2 + \left(1 - \text{Fr}^2 + \frac{1}{2} C_T B \text{Fr}^2 \right) \times \frac{\Delta h}{h} - \frac{1}{2} C_T B \text{Fr}^2 = 0$$

The far-field change in the free surface elevation characterises the far-field impact of energy extraction from the open channel, and may be of interest when assessing the performance of tidal turbines. It is informative to introduce an additional efficiency measure, the basin efficiency, which supplements the traditional efficiency described by the power coefficient.

The total power removed from the channel, found as the difference in energy flux between stations 1 and 5, may be expressed as the difference in total head $H_1 - H_5$ between the two stations

$$20. \quad P_{\text{Tot}} = g \rho b h u (H_1 - H_5)$$

where $\rho b h u$ is the mass flow rate through the channel, $H_1 = h_1 + (1/2)(u_1^2/g)$ and $H_5 = h_5 + (1/2)(u_5^2/g)$. The total power dissipated in the channel can thus be expressed as

$$21. \quad P_{\text{Tot}} = \rho g b h \Delta h \left(1 - \text{Fr}^2 \frac{1 - (1/2)(\Delta h/h)}{(1 - (\Delta h/h))^2} \right)$$

The basin efficiency defined in Equation 6 may therefore be expressed as

$$22. \quad \eta = \frac{\alpha_2 \left((1 - (\Delta h/h))^2 (1 - (1/2)(\Delta h/h)) - \text{Fr}^2 (1 - (\Delta h/h)) \right)}{\left((1 - (\Delta h/h))^2 - \text{Fr}^2 (1 - (1/2)(\Delta h/h)) \right)} = \frac{\alpha_2 C_T}{C_{P\text{Tot}}}$$

For many tidal flows, $\text{Fr}^2 \ll 1$, so that the total power removed from the channel, to the first order, may be approximated as $P_{\text{Tot}} = \rho g b h u \Delta h$. When the Froude number is small, the basin efficiency may be approximated as

$$23. \quad \eta = \alpha_2 \left(1 - \frac{1}{2} \frac{\Delta h}{h} \right)$$

At small Froude numbers, the basin efficiency may thus be primarily described in terms of the non-dimensional velocity α_2 , with a small correction for the deformation of the free surface which acts to reduce the basin efficiency for a given α_2 .

Critical flow in the bypass corresponds to the condition in which the derivative of the energy function with respect to h_4 is zero, $dE_4/dh_4 = 0$, which defines the point at which h_4 is so small that energy is only just conserved in the bypass. Further reduction of h_4 results in the back-up of flow and in the possibility of development of a hydraulic jump. Energy conservation in the bypass stream tube requires

$$24. \quad \frac{dE}{dh_4} = \frac{d}{dh_4} \left(\frac{1}{2} \frac{u^2}{g} \beta_4^2 + h_4 \right) = \frac{1}{2} h \text{Fr}^2 \frac{d}{dh_4} \beta_4^2 + 1 = 0$$

Evaluating the derivative leads to

$$25. \quad \frac{d(\beta_4^2)}{dh_4} = - \frac{2}{h \text{Fr}^2}$$

which corresponds to the point at which physically admissible solutions to Equation 17 cease to exist. The lack of a physical

solution for an open channel flow may imply the onset of critical flow at some point in the flow field, and means that Equation 17 is not guaranteed to have a solution for general values of B and Fr .

2.3 Limiting cases

If $\Delta h/h$ is small, then the cross-sectional area is constant along the length of the channel. Neglecting the high-order $\Delta h/h$ terms in Equation 19 yields an expression for $\Delta h/h$

$$26. \quad \frac{\Delta h}{h} = \frac{Fr^2 BC_T}{2 + Fr^2(BC_T - 2)}$$

Thus, taking $Fr^2 \rightarrow 0$, it can be seen that $\Delta h/h \rightarrow 0$, and therefore the limit of the generalised open channel model is the rigid-lid model derived by Garrett and Cummins (2007).

The Froude number represents the relative balance between dynamic and static head in the flow, and thus $Fr^2 \rightarrow 0$ indicates that the dynamic energy in the flow is negligible relative to the static energy, and therefore the effect of the thrust on the kinetic energy is negligible relative to the effect on the static energy. Therefore, in the limit $Fr^2 \rightarrow 0$, only the hydrostatic pressure changes far downstream of the actuator disc and there is negligible change in the flow speed between the channel inlet and outlet.

Neglecting the free surface deformation and the attendant changes in the cross-sectional area of the channel allows a number of simplifications to be made to the generalised model, and hence the rigid-lid model requires the solution of only a quadratic in β_4 rather than a quartic as in the present model.

A second limiting case is found when the channel width $b \rightarrow \infty$, so that $B \rightarrow 0$, and the actuator disc occupies an infinitesimal fraction of the channel cross-section. Conservation of mass in the bypass stream tube requires

$$27. \quad \beta_4 = \frac{bh - A_{d1}}{bh - A_{d4}}$$

Thus, as $b \rightarrow \infty$, $\beta_4 \rightarrow 1$. In this limit, Equation 13 becomes

$$28. \quad T = \rho u^2 A \alpha_2 (1 - \alpha_4)$$

Combining Equation 28 with Equation 12, it can be shown that the unblocked actuator disc analysis of Lanchester (1915) and Betz (1920) is recovered, where the relationship between α_2

and α_4 is given by

$$29. \quad \alpha_2 = \frac{1}{2}(1 + \alpha_4)$$

3. Results

Figures 2 and 3 show the effect of blockage on the power coefficient and basin efficiency at Froude number representative of some sites of interest for the extraction of tidal power, such as the Severn Estuary, $Fr = 0.20$. Increasing the blockage ratio results in a higher peak power coefficient, as shown in Figure 2, where the peak C_P increases from 0.66 at $B = 0.05$ to 1.29 at $B = 0.30$. Peak C_P is achieved at higher thrust levels as the blockage ratio increases, with the thrust coefficient increasing from 1.02 at $B = 0.05$ to 2.67 at $B = 0.30$. Note that there is no contradiction in values of C_P which is greater than unity, as the undisturbed kinetic power flux is simply a reference value, not a limit of the power available to the device.

The increase in peak C_P and C_T occurs because an increasingly large static head difference is established in the confined flow passage around the actuator disc, allowing a greater thrust to be applied at a given through-disc flow speed, or equivalently, a higher flow speed through the actuator disc for a given thrust. As the available power is calculated from the product of thrust and through-disc flow speed, C_P increases in both circumstances, and the rate of increase in peak C_P also increases with blockage ratio. Preliminary qualitative experimental evidence to support this has been reported by Cooke *et al.* (2015), exploring the relationship between turbine spacing, thrust and

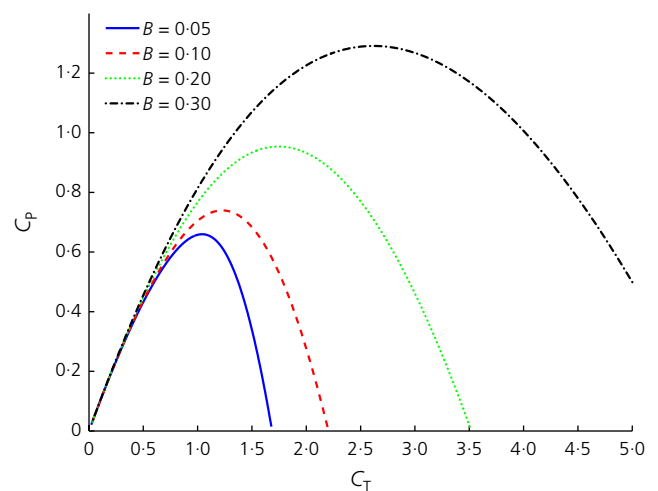


Figure 2. C_T against C_P for four blockage ratios: $B = 0.05$ (solid), $B = 0.10$ (dashed), $B = 0.20$ (dotted), $B = 0.30$ (dash-dotted). $Fr = 0.20$ for all cases

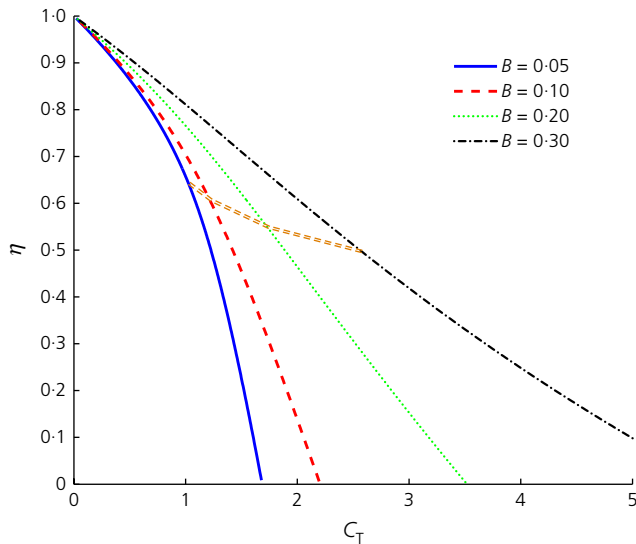


Figure 3. C_T against η for four blockage ratios: $B=0.05$ (solid), $B=0.10$ (dashed), $B=0.20$ (dotted), $B=0.30$ (dash-dotted). $Fr=0.20$ for all cases. η at peak C_p is plotted with the double dashed line

power, for actuator discs in a flume tank. Further actuator disc experiments, including the measurement of free surface height, would be required to make a full comparison with the results presented herein.

The increase in flow speed through the actuator disc at a given level of thrust as blockage increases is demonstrated in Figure 3. At a given C_T , basin efficiency is higher as blockage increases, as the higher flow speed (and therefore mass-flux) through the actuator disc, and consequently through the core stream tube, means that the flow speed in the bypass stream tube is lower. This reduces the shear stresses that develop as a result of the velocity differential in the two stream tubes, reducing the intensity of mixing, and therefore dissipating less power, in the wake of the disc. It then follows from Equation 6 that the basin efficiency is higher, as a greater fraction of the power removed from the flow is available to the actuator disc.

As the blockage ratio increases, the basin efficiency achieved at peak C_p decreases, as shown by the double dashed line in Figure 3. Although at a given C_T , higher blockage discs are more efficient, the larger thrust that can be supported in higher blockage regimes results in a larger difference in bypass and core flow speeds, resulting in greater shear stresses and therefore mixing losses in the mixing region.

Figures 4 and 5 show the effect of Froude number on the power coefficient and basin efficiency for a typical blockage

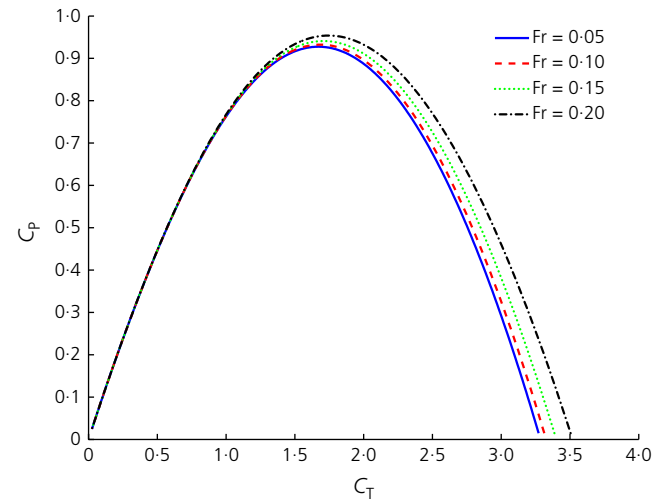


Figure 4. C_T against C_p for the four Froude numbers: $Fr=0.05$ (solid), $Fr=0.10$ (dashed), $Fr=0.15$ (dotted), $Fr=0.20$ (dash-dotted). $B=0.20$ for all cases

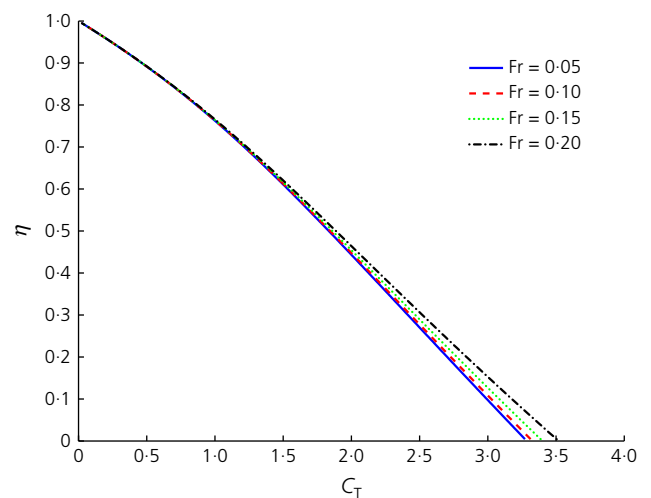


Figure 5. C_T against η for the four Froude numbers: $Fr=0.05$ (solid), $Fr=0.10$ (dashed), $Fr=0.15$ (dotted), $Fr=0.20$ (dash-dotted). $B=0.20$ for all cases

ratio, $B=0.2$. Increasing the Froude number from 0.05, typical of a low-flow-speed, deep-sea site, to 0.20, typical of a shallower, higher-flow-speed site, results in the peak C_p increasing from 0.93 to 0.95, an increase of 3%. Basin efficiency also increases slightly as the Froude number increases, with the efficiency improvement becoming more significant at higher thrust coefficients. Deformation of the channel free surface increases as the Froude number increases, further constraining

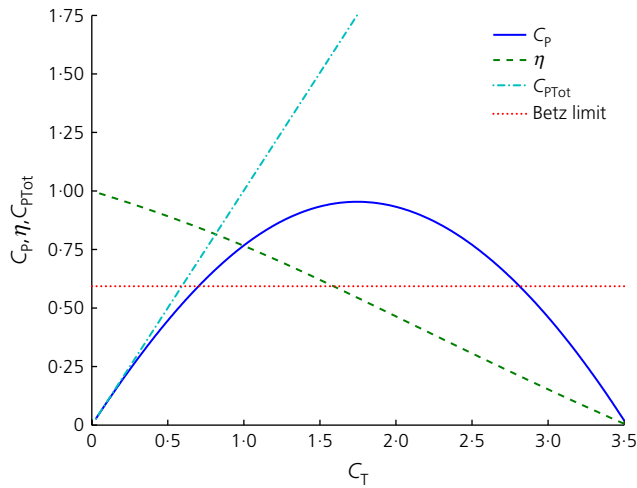


Figure 6. C_T against C_P (solid), η (dashed) and C_{PTot} (dot-dashed) for $B=0.20$, $Fr=0.20$. The Betz (1920) limit is illustrated with a dotted line

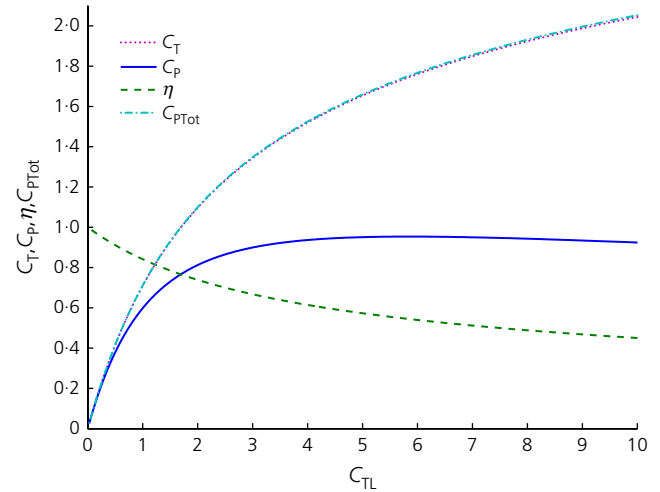


Figure 7. C_{TL} against C_T (dotted), C_P (solid), η (dashed) and C_{PTot} (dot-dashed) for $B=0.20$, $Fr=0.20$

the flow passage, thus increasing the static head difference that forms in the channel, with the same effect on the thrust and flow speed through the actuator disc as the blockage ratio has, albeit to a lesser extent. Basin efficiency reduces slightly as the Froude number increases, reducing from 0.56 at $Fr=0.05$ to 0.54 at $Fr=0.20$.

Figure 6 plots C_P , η and C_{PTot} for $B=0.20$ and $Fr=0.20$, typical of a tidal turbine in a relatively closely packed array in a shallow channel, and illustrates the compromise that must be achieved between power coefficient and basin efficiency. Peak C_P is achieved at a basin efficiency of 0.54, and a C_{PTot} of 1.84, which means that 1 MW of available power requires 1.84 MW to be removed from the flow. Removing a significant amount of power from the flow may significantly change sediment dynamics and pollution dispersion, and alter the marine environment, and therefore regulators may limit turbines to some minimum basin efficiency. Choosing to operate at a basin efficiency of 0.90 or greater would, however, result in a very low power coefficient, and the small level of available power may mean it is not economical to deploy tidal turbines. Consequently, a compromise is required between the use of the overall tidal resource (basin efficiency) and the output of each turbine (power coefficient) in order to satisfy environmental and regulatory requirements while achieving economically feasible levels of power extraction from the tidal flow.

The effect of device design is illustrated in Figure 7, which compares C_T , C_P , η and C_{PTot} as C_{TL} varies for $B=0.20$ and $Fr=0.20$. The local thrust coefficient, C_{TL} , is a measure of the

effect of power removal on the flow close to the device, and also informs design decisions about the level of thrust, for example, that is to be expected by the device. An optimal wind turbine operating at the Betz (1920) limit of $C_P=0.593$ has $C_{TL}=2$, whereas the tidal device achieves $C_P=0.813$ when $C_{TL}=2$. The improved power coefficient is a result of flow confinement by the free surface and the head difference established in the channel as a result of power extraction by the device, which increases the flow speed through the device for a given applied thrust, consequently increasing the available power.

Fully exploiting the increased power available to tidal devices as compared with wind turbines requires that the tidal devices present a greater thrust to the flow than wind turbines. The peak power coefficient for a tidal device with a blockage $B=0.20$ and $Fr=0.20$ is $C_{P,Peak}=0.954$, which is achieved with a local thrust coefficient $C_{TL}=5.85$, almost three times greater than that of an idealised wind turbine, which would require a significantly strengthened structure to achieve, with an attendant increase in design and construction costs. At this operating point, the thrust coefficient is $C_T=1.75$, and the basin efficiency $\eta=0.54$. Designing the device to achieve 90% of the peak power coefficient, $C_P=0.859$, reduces the local thrust coefficient to $C_{TL}=2.429$, 41.5% of the local thrust coefficient required to achieve the peak power coefficient. The basin efficiency is improved by 29.6% to $\eta=0.71$, and the thrust coefficient is reduced by 30.5% to $C_T=1.218$. It is noted that C_T and C_{PTot} remain approximately equal as C_{TL} increases, as a result of the small free surface deformation of the flow. To a first-order approximation, the Fr^2 terms in Equation 22 are small, allowing the ratio of C_T to C_{PTot} to be

		Number of turbines				
		1	10	50	100	500
Shallow channel	Blockage	0.0175	0.175	0.8727	—	—
	Power/turbine: MW	2.68	3.887	5.704	—	—
	Thrust/turbine: MN	1.364	2.316	1.937	—	—
	Basin efficiency	0.653	0.5578	0.9694	—	—
Deep channel	Blockage	0.000698	0.007	0.0349	0.0698	0.349
	Power/turbine: MW	0.764	0.776	0.82	0.883	1.838
	Thrust/turbine: MN	0.573	0.586	0.636	0.709	1.881
	Basin efficiency	0.6665	0.6623	0.6443	0.6231	0.4872

Table 1. Comparison of turbine power, thrust and basin efficiency for a single row of tidal turbines in representative shallow and deep tidal channels

approximated as

$$30. \quad \frac{C_T}{C_{PTot}} = 1 - \frac{1}{2} \frac{\Delta h}{h}$$

Consequently, for small free surface deformations, the thrust coefficient and total power coefficient remain approximately equal.

Table 1 summarises the results of the analytical model for two tidal channels, a shallow channel and a deep channel, representative of regions where tidal current turbines are being considered for deployment. The shallow channel is representative of Strangford Lough, with a uniform depth of 30 m, and width of 600 m. The flow speed is assumed to be 3 m/s, which gives a Froude number $Fr = 0.2$. The deep channel is representative of the Pentland Firth, with a uniform depth of 50 m, width of 9 km and a flow speed of 2 m/s, giving a Froude number of $Fr = 0.1$. The turbines have a diameter of 20 m, and are assumed to be arranged in a single row uniformly spaced across the channel and it is assumed that the flow speed through the channel is unchanged, an assumption that is unlikely to hold for large numbers of turbines, and that can be relaxed by considering the head driving the flow through the channels as described by Garrett and Cummins (2005). The power available per turbine increases as the number of turbines (and therefore blockage) increases in both cases, with more power being generally available to turbines in the shallow channel for a given blockage on account of the higher flow speed. However, the power-to-thrust ratio and basin efficiency decreases as the blockage increases, which means more structurally resilient turbines that extract power less efficiently from the overall tidal resource are required to achieve the higher

levels of power as the blockage ratio increases. The exception to this is the highest blockage case in the shallow channel, where high basin efficiency is achieved because the model solution becomes unphysical as the turbine resistance is increased further.

Achieving the theoretical peak power available to tidal devices may be technically challenging due to the high structural loads required to achieve peak power, and the modest corresponding basin efficiency indicates that a large amount of additional power must be removed from the flow in order to access the theoretical peak available to the devices. Slightly reducing the power to be achieved by the turbines may result in significant improvements in the utilisation of the tidal resource (basin efficiency), and also significantly reduce the local thrust coefficient to a level comparable to that expected by an idealised wind turbine.

4. Conclusions

An analytical model has been developed by extending LMADT for wind turbines and tidal turbines in rigid-lid channels to tidal turbines in an open channel, allowing the effect of energy extraction to be investigated in sub-critical tidal flows. The model allows the performance of a tidal turbine to be estimated in a number of different blockage and flow conditions.

The peak power coefficient is strongly related to blockage, and to the Froude number to a lesser extent, increasing significantly above the Betz (1920) limit as the blockage ratio increases. Higher peak power coefficients are achieved as the blockage ratio increases because the head difference that develops in the channel allows a greater thrust to be exerted on the flow. However, this reduces the basin efficiency of the turbine, causing more power to be dissipated in the mixing processes

downstream of the turbine. It will therefore be necessary to balance environmental concerns about energy extraction with the power available to turbines in order to ensure that environmental consequences are mitigated while also achieving economic power extraction.

The blockage ratio is a very significant parameter for device developers, and the present model demonstrates that significant improvements in device performance may be achieved at realistic blockage ratios. At $B=0.20$, peak C_P is 0.95, representing a 60% improvement on the Betz (1920) limit. This blockage ratio could be achieved by an axial flow turbine in a flow passage 2 diameters deep with an inter-turbine spacing of 2 diameters, or a cross-flow turbine in a flow passage 5 diameters deep.

Introducing the concept of basin efficiency, the ratio of power available to the turbines to the total power removed from the flow suggests that turbines could be operated in a manner which balances the environmental impacts of energy extraction with the power available to the devices. The environmental impact of energy extraction may be reduced by operating the devices at, for example, 90% of peak C_P , which increases the basin efficiency from 54 to 71% for turbines which occupy 20% of the channel cross-section, making better use of the tidal resource. Targeting a slightly lower C_P value has the advantage of significantly reducing the thrust required to be applied to the flow. In this case, the local thrust coefficient reduces from $C_{TL}=5.85$ to 2.43, substantially reducing the structural loads on the turbine. This may play a very important role in improving the technological and commercial feasibility of tidal devices. Additional benefits arise from the smaller, cheaper generators required to achieve the lower levels of power, suggesting that designing turbines to achieve power levels slightly below optimum may yield a range of benefits for tidal turbine developers.

Acknowledgements

The authors acknowledge Professor Martin Oldfield and Associate Professor Scott Draper for their inputs in the development of the analysis.

REFERENCES

- Adcock TAA, Draper S, Houlsby GT, Borthwick AGL and Serhadgloğlu S (2014) Tidal stream power in the Pentland Firth – long-term variability, multiple constituents and capacity factor. *Proceedings of the Institution of Mechanical Engineers, Part A: Journal of Power and Energy* **228(8)**: 854–861.
- Adcock TAA, Draper S and Nishino T (2015) Tidal power generation – a review of hydrodynamic modelling. *Proceedings of the Institution of Mechanical Engineers, Part A: Journal of Power and Energy* **229(7)**: 755–771.

- Betz A (1920) Das maximum der theoretisch moglichen Ausnutzung des windes durch windmotoren. *Zeitschrift für das gesamte Turbinenwesen* **26**: 307–309 (in German).
- Bryden IG, Couch SJ, Owen A and Melville G (2007) Tidal current resource assessment. *Proceedings of the Institution of Mechanical Engineers, Part A: Power and Energy* **221(2)**: 125–135.
- Cooke SC, Willden RHJ, Byrne BW, Stallard T and Olczak A (2015) Experimental investigation of tidal turbine partial array theory using porous discs. *Proceedings of the 11th European Wave and Tidal Energy Conference (EWTEC), Nantes, France*, pp. 09D2-5-1–09D2-5-10.
- Carbon Trust (2007) *Future Marine Energy*. Carbon Trust, London, UK.
- Carbon Trust (2010) *UK Tidal Current Resource and Economics*. Carbon Trust, London, UK.
- Garrett C and Cummins P (2005) The power potential of tidal currents in channels. *Proceedings of the Royal Society A* **461(2060)**: 2563–2572.
- Garrett C and Cummins P (2007) The efficiency of a turbine in a tidal channel. *Journal of Fluid Mechanics* **588**: 243–251.
- Houlsby GT, Draper S and Oldfield MLG (2008) *Application of Linear Momentum Actuator Disc Theory to Open Channel Flow*. University of Oxford, Oxford, UK, Report OUEL 2296/08.
- Kirby R and Retière C (2009) Comparing environmental effects of Rance and Severn Barrages. *Proceedings of the Institution of Civil Engineers – Maritime Engineering* **162(1)**: 11–26, <http://dx.doi.org/10.1680/maen.2009.162.1.11>.
- Lanchester F (1915) A contribution to the theory of propulsion and the screw propeller. *Transactions of the Institute of Naval Architects* **57**: 98–116.
- Whelan JJ, Graham JMR and Peiró J (2009) A free-surface and blockage correction for tidal turbines. *Journal of Fluid Mechanics* **624**: 281–291.

HOW CAN YOU CONTRIBUTE?

To discuss this paper, please email up to 500 words to the editor at journals@ice.org.uk. Your contribution will be forwarded to the author(s) for a reply and, if considered appropriate by the editorial board, it will be published as discussion in a future issue of the journal.

Proceedings journals rely entirely on contributions from the civil engineering profession (and allied disciplines). Information about how to submit your paper online is available at www.icevirtuallibrary.com/page/authors, where you will also find detailed author guidelines.